

Simulation and Robot Implementation of Visual Orientation Behaviors of Flies

Susanne A. Huber, Heinrich H. Bülthoff

Max-Planck-Institut für biologische Kybernetik

Spemannstr. 38, 72076 Tübingen, Germany.

susanne.huber@tuebingen.mpg.de

heinrich.buelthoff@tuebingen.mpg.de

Abstract

Flies have developed visuomotor programs for tasks like course stabilization, fixation and approach towards stationary objects, tracking of moving objects, and landing, which are based on the analysis of visual motion information. Theoretical and experimental results suggest that the visuomotor control for course stabilization as well as fixation and approach towards stationary objects may be realized at least partially by one common sensory circuit. In order to test this hypothesis we designed simulated agents, with a control architecture that is based on results from fly research. We present agents with a visuomotor controller that regulates the two behaviors of course stabilization and object fixation. To test this controller under real world conditions, we implemented it on a miniature robot. We can show that besides course stabilization and object fixation, the robot additionally approaches stationary objects.

1. Introduction

Researchers have been attracted to the field of insect research for many years, because insects show stimulus-response characteristics that allow insight into the mechanisms of visual information processing as well as into the interaction of sensory input and motor output. Especially the visually controlled orientation behavior of flies is particularly well studied (Reichardt and Poggio, 1976; Heisenberg and Wolf, 1984; Egelhaaf and Borst, 1989).

A promising approach to help to understand information processing in living systems is the study of artificial systems and their interaction with the environment. The simulation of biological systems and the implementation of behavioral models (Tinbergen, 1953; Brooks, 1986) onto robots seems to be especially useful to the understanding of biological systems. Several examples exist where researchers implemented sensorimotor mechanisms of insects into robots (e.g., Beer, 1990; Cliff, 1992; Cruse, Bartling, Cymbalyk, Dean, and Deifert, 1995; Webb, 1995). Orientation mechanisms inspired by the behavior of flies have been implemented in computer simulation or on mobile robots. For example, visuomotor

controllers have been designed that use visual motion information. Mostly these agents use the visual motion information for obstacle avoidance (Franceschini, Pichon, and Blanes, 1992; Duchon and Warren, 1994; Weber, Venkatesh, and Srinivasan, 1997) or tracking of other objects (Cliff, 1992; Missler and Kamangar, 1995).

Results from fly research suggest that the two behaviors of course stabilization and approach towards stationary objects may be realized at least partially by one common behavioral module (Götz and Wenking, 1973; Götz, 1975; Reichardt and Poggio, 1976; Bülthoff, 1982). We use the robotics approach to investigate this hypothesis. Our goal is to build a single visuomotor controller that regulates both behaviors. We modeled the subsequent processing steps in the visual system of flies in detail. Like the robots of Franceschini et al. (1992) and others, the agent uses visual motion information of a 360° horizontal field of view for behavior control. We can demonstrate that our computer-simulated agent is able to control the two behaviors of course stabilization and approach towards stationary objects by evaluating the motion information with a single visuomotor controller. To test the behaviors under real world conditions, we implement the control structure on a miniature robot – the *KheperaTM* (Mondada, Franzi, and Ienne, 1994).

2. The agent's architecture

2.1 Model of the visual system

We implemented a simplified model (Fig. 1) of visual information processing in flies, i.e. contrast enhancement, reduction of signal redundancy, signal amplification, motion detection and evaluation of the motion signals which takes place in the subsequent neural layers lamina (L), medulla (M) and lobula plate (LP) in the visual section of the fly's brain.

Spatial and temporal lowpass filtering in the retina: The agent has a horizontal array of sensors with a 360° field of view which scans the visual world at the horizon. By ray-tracing, the simulated agent determines (Foley, van Dam, Feiner and Hughes, 1987), the inten-

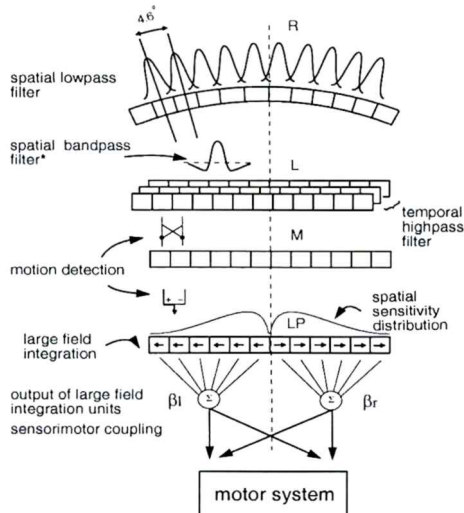


Figure 1 *Model of the visuomotor controller with the functional processing steps that take place in the different layers of the agent's visual system (*the bandpass filter is only realized on the KheperaTM robot, see Section 4.).*

sities of 780 single points which are equally distributed over the 360° horizontal field of view, at the intersections of the lines of sight with the visible surfaces (for the robot implementation see Section 4.). Second, these samples are spatially lowpass filtered by Gaussian filters ($\sigma = 3.8^\circ$) Like in *Drosophila* (Götz 1964), the sensors have an interommatidial angle of $d\varphi = 4.6^\circ$. Hence the array has 78 sensors.

Redundancy reduction and amplification of the signal in the lamina: In *Drosophila* large monopolar cells (LMCs) in the lamina are known to be responsible for signal amplification, local contrast enhancements and reduction of redundant parts of the signal (Laughlin 1987). In this work we modeled the temporal aspects of the LMC cells by applying a temporal highpass filter H ($\tau_H = 20.0$ steps), which eliminates parts of the signal that are steady or slowly changing in time. In a next step the signals are linearly amplified to the full range of 256 grey-level values.

Motion detection in the medulla and lobula plate:

For motion perception in insects, Hassenstein and Reichardt (1956) proposed a detector which correlates temporal modulation of image intensities in two neighboring ommatidia. The detector model has two mirror-symmetrical subunits. In each subunit the signals of two input channels are multiplied after the signals have been delayed by two lowpass filters with different time constants ($\tau_1 = 1.5$ steps and $\tau_2 = 5.0$ steps). In a next step the outputs of the two subunits are subtracted to obtain the direction of the motion stimulus.

Integration of the motion signals in the lobula plate: In the fly's lobula plate neurons have been described which are specialized to certain motion patterns. For example the HSE cells receive input from motion detectors that respond stronger to a pattern moving from front to back (progressive motion) than from back to front (regressive motion). The asymmetry results, because the time course of these motion detector subunits is not completely mirror symmetric (Egelhaaf, Borst and Reichardt 1989). This is modeled by a gain of 1.0 for progressive and 0.7 for regressive motion. In addition the horizontal equatorial cells (HSE cells) respond maximal to horizontal progressive motion in the frontolateral field of view (Hausen 1982). Modeling the HSE cells, two large field units integrate the motion information over a 184° field of view in the right and left hemisphere with an overlapping region of 8° in the front. The sensitivity distribution $S(j)$ (j number of sensor¹) is modeled by the function:

$$S(j) = aj^b e^{-cj} \quad (1)$$

with $a = 0.625$, $b = 0.7$ and $c = 0.15$ and $j \in [-1, 39]$. $S(j)$ is bilaterally symmetrical for the two integration units ($S(j) = S(-j)$) and the maximum of $S(j)$ is at the sensor 5 (at $\varphi_{\max} = 23^\circ$). The outputs (β_l, β_r) of the integration units are coupled via transmission weights to the motor system.

2.2 Model of the motor system:

The agent is modeled as a simple kinematic system with two motors, ignoring its mass and inertia. In order to model the visuomotor control of flies this approximation can be made, because after an initial acceleration, within a short time (< 10 ms) the fly reaches a constant velocity as the force produced by the wings is balanced by the increasing air friction. The motors have a distance of $c = 1u$, given in units u of the agent's size ($1u = 0.25$ cm).²

The velocities v_l and v_r (Fig. 2) of the motors are proportional to the force of the two motors. Each motor produces a constant velocity $v_0 = 0.1$ u/step which is modulated by the outputs of the processed visual information:

$$v_{l,r} = v_0 - T(s_{l,r}) \quad (2)$$

The signals s_l and s_r result from the visual motion information via the control signals m_l and m_r and intrinsic noise n_l and n_r (Fig. 3):

$$s_{l,r} = km_{l,r} + n_{l,r} \quad (3)$$

¹ The sensors ± 1 are oriented at the visual angles $\varphi = \pm 2.3^\circ$ off the heading direction and the sensors ± 39 at $\varphi = \pm 177.1^\circ$

² The force vectors produced by the wings of the fruitfly *Drosophila* have an estimated perpendicular distance from the center of the fly of about 0.2 to 0.3 cm (body-length: 0.3 cm) (Götz, 1964).

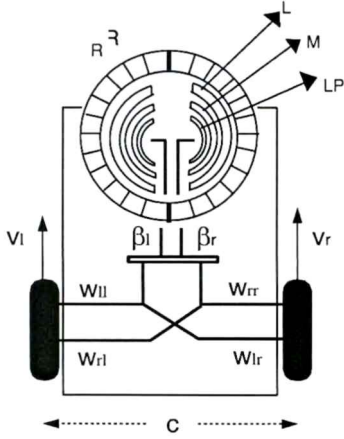


Figure 2 Sketch of the agent with ring sensor (R), simplified models of the three layers of the visual system: lamina (L), medulla (M), lobula plate (LP), and the transmission weights ($w_{ll}, w_{lr}, w_{rl}, w_{rr}$) that couple the outputs of the large field units (β_l, β_r) to the motor system.

where k is a proportionality factor. The control signals m_l and m_r are explained in detail in the next section. As the force produced by the wings of the fly never becomes negative, the velocities v_l and v_r are always above or equal 0 u/step. This is achieved by the sigmoid function $T(s)$ for the left and right motor respectively:

$$T(s) = \begin{cases} -v_0 & \text{if } s < -v_0, \\ s & \text{if } |s| \leq v_0, \\ v_0 & \text{if } s > v_0, \end{cases} \quad (4)$$

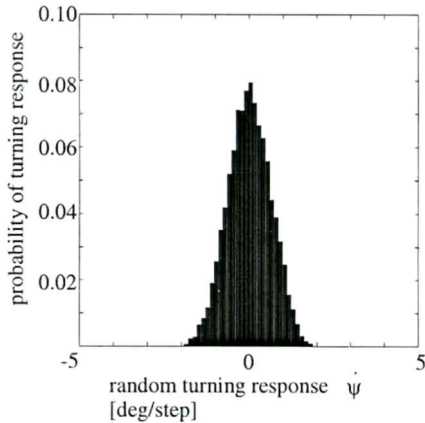


Figure 3 Noise signal n_l of left motor (Gaussian distributed with $\sigma = 0.64^\circ/\text{step}$).

The system has two degrees of freedom: translation in the heading direction and rotation around the vertical body-axis. The translatory and rotatory velocities are:

$$v_t = \frac{v_r + v_l}{2} \quad \text{and} \quad \dot{\psi} = \frac{v_r - v_l}{c}. \quad (5)$$

2.3 The sensorimotor coupling

Fixation behavior: Reichardt and Poggio (1976) showed in behavioral studies with flies that a fly orients itself towards a single black stripe in an otherwise homogeneous arena. This so-called fixation behavior is in contrast to the behavior in a visually homogeneous environment, where a fly turns in all directions with equal probability. Due to intrinsic noise the motor system continuously produces torque, resulting in turning movements in either direction. Reichardt and Poggio (1976) showed that the noise is Gaussian distributed.

One explanation of the fixation behavior is based on the fact that the turning response of flies in open-loop experiments is stronger if a stripe moves from front to back than in the other direction (Heisenberg and Wolf, 1984), due to the asymmetric response of the HS-neurons. As the noisy torque signals of the motor system lead to movements of an object's retinal image, the resulting image flow will cause the fly to orient towards the object, because the positive response to progressive motion is stronger than the negative response to regressive motion.

To model the fixation behavior of flies, the signals that result from the large field integration are coupled proportionally to the motor system.

$$\begin{aligned} m_l^f(t) &= \omega_{ll}\beta_l + \omega_{lr}\beta_r \\ m_r^f(t) &= \omega_{rl}\beta_l + \omega_{rr}\beta_r. \end{aligned} \quad (6)$$

The matrix

$$\mathbf{W} = \begin{pmatrix} \omega_{ll} & \omega_{lr} \\ \omega_{rl} & \omega_{rr} \end{pmatrix} = \begin{pmatrix} 0.9 & -0.4 \\ -0.4 & 0.9 \end{pmatrix} \quad (7)$$

contains the transmission weights for the coupling of the outputs β_l and β_r of the two large field integration units to the left and right motor. We assume bilateral symmetry for the sensorimotor coupling.

Optomotor response: While flying, flies are continuously stabilizing their course. In order to compensate for disturbances, which cause large rotatory image motion, they execute turning movements – the so-called optomotor response – along the direction of the image motion. This behavior is most probably realized by cells that continuously integrate the difference of the output signals from the horizontal cells in the two optic lobes (Heisenberg and Wolf, 1984). A motor signal, purely proportional to the difference of the image motion in the two eyes, has the disadvantage that ambiguous motor signals result with respect to pattern velocity. This is due to the characteristic response of the Reichardt motion detector, which increases with increasing image motion up to an optimum and decreases again for faster motion. It is impossible to decide whether the image motion resulted from a pattern that moves at low or very high

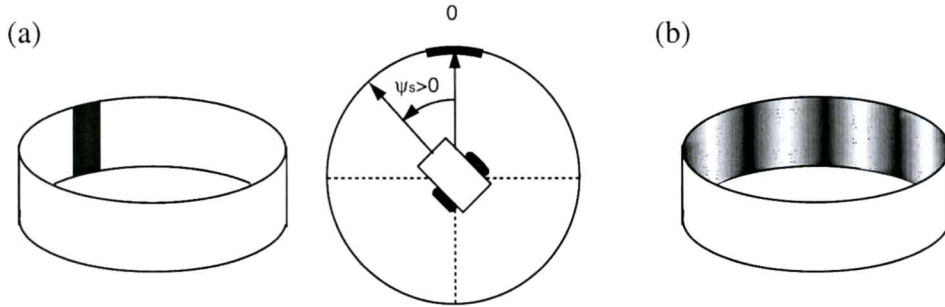


Figure 4 Sketch of simulated arena. (a) side and top view of the arena with one black stripe mapped onto the wall. The stripe is at 0° , starting orientation of agent is at ψ_s . (b) A sinusoidal pattern is mapped onto the wall.

speed and full compensation is not possible. In general, a purely proportional controller (without memory) may cause oscillations, because the compensation behavior is active only until the retinal image is stabilized. As the disturbance persists, image flow will be detected again and the compensation behavior is active again until the retinal image is stabilized again etc. This second point, however, does not seem to be a disadvantage for the control system of flies. Warzecha and Egelhaaf (1996) could show that due to the response characteristic of the motion detector large-amplitude fluctuations in the image motion, which are generated when the optomotor system gets unstable, are transmitted with a small gain leading to only relatively small turning responses and thus small image motion.

To model the optomotor response behavior, the signals β_l and β_r that result from the large field units are integrated over time. In simulation the integration is replaced by a summation:

$$B_{l,r}(t) = \sum_{-\infty}^t \beta_{l,r}(t') \quad (8)$$

The coupling of these signals to the motor system, leads to the control signals:

$$\begin{aligned} m_l^{or}(t) &= \omega_{ll} B_l(t) + \omega_{lr} B_r(t) \\ m_r^{or}(t) &= \omega_{rl} B_l(t) + \omega_{rr} B_r(t) , \end{aligned} \quad (9)$$

with the transmission weights from Eq. 7.

Optomotor response and object fixation: Experimental results suggest that the behaviors for course stabilization and approach towards stationary objects of flies may be realized at least partially by a common sensory circuit (Götz and Wenking, 1973; Götz, 1975; Reichardt and Poggio, 1976; Bühlhoff, 1982). In order to test this we designed agents with a visuomotor controller, that regulates both the optomotor response and the fixation behavior.

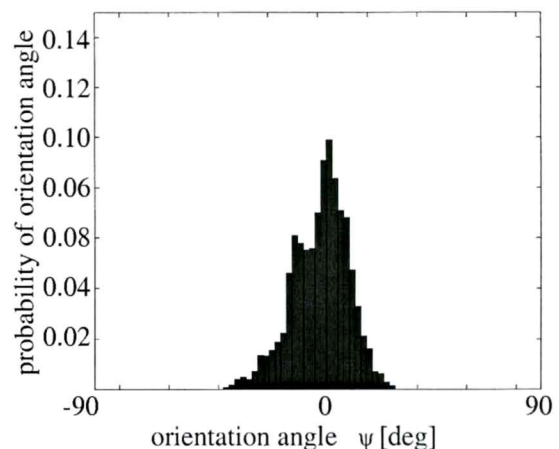


Figure 5 Histogram of the agent's orientation angle ψ in a drum: with one stripe at $\psi_s = 0.0^\circ$: $\bar{\psi} = 0.95^\circ \pm 11.21^\circ$.

For the controller the control signals for optomotor response m_{or} and object fixation m_f are combined into a proportional-integral controller:

$$m_{l,r}(t) = k_f m_{l,r}^f(t) + k_{or} m_{l,r}^{or}(t) , \quad (10)$$

with the constant factors $k_f = 0.5$ u/step and $k_{or} = 5.0 \cdot 10^{-4}$ u/step.

3. Experiments with the simulated agent

3.1 Fixation behavior

To compare the performance of the fixation behavior of the agent with that of flies in the experiments of Reichardt and Poggio (1976), we run three experiments. In all three experiments, the agent is fixed in the middle of a drum and therefore has only one degree of freedom, the rotation around its vertical body axis (Fig. 4a). The angular velocity of the turning response $\dot{\psi}$ is given by Eq. 5.

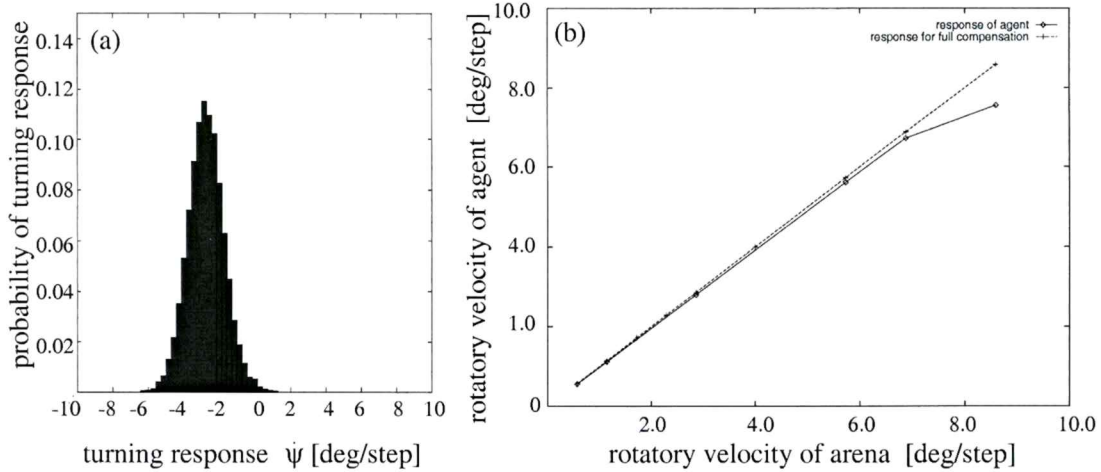


Figure 6 *Optomotor response: (a) Histogram of the agent's optomotor response. The agent is fixed at the center of a rotating drum. Rotation of drum: $\dot{\psi}_d = 2.9^\circ/\text{step}$; rotation of agent: $\dot{\psi} = 2.8 \pm 1.0^\circ/\text{step}$. (b) The agent's optomotor response in dependency of the angular speed of the arena.*

Experiment: A single black stripe (angular width 17.3°) is presented on the wall of the drum in an otherwise white surrounding. The initial orientation of the agent is $\psi_s = 41.4^\circ$. The simulation runs for 10,000 time steps.

Result: Due to random torques caused by intrinsic noise of the system, the retinal image of the stripe is not stationary. The agent turns towards the object, because the turning response is stronger to progressive than to regressive motion. Within 1100 steps the agent orients its heading direction towards the stripe. For the rest of the simulation the agent is able to fixate on the stripe (Fig. 5). The slightly overlapping receptive fields of the integration units are necessary for the agent to keep the stripe in the front, because agents which lack this characteristic are not able to fixate on the stripe in front of them.

3.2 Optomotor response behavior

Experiment: Like in the previous experiment, the agent is fixed in the middle of a drum (Fig. 4b) and can only turn around its vertical body axis. In order to test the optomotor response a sinusoidal pattern ($\lambda = 36^\circ$) rotates with a constant angular velocity $\dot{\psi}_d$. The simulations run for 10,000 time steps with different velocities $\dot{\psi}_d$ (Fig. 6b).

Results: In order to stabilize the retinal image and thus its orientation in the drum, the agent produces on average a compensatory turning response of $\dot{\psi} \pm \sigma_{\dot{\psi}}$ (Fig. 6). The agent is able to compensate for 97% of the arena's rotation if the angular velocity is lower than $7^\circ/\text{step}$.

Due to the sigmoid function (Eq. 4) the agent is not able to compensate to this extent for higher velocities of the drum.

Experiment: Due to the response characteristic of the Reichardt motion detector, a purely proportional controller, does not lead to an unstable behavior, we also test the performance of the agent with a purely proportional controller (Warzecha and Egelhaaf, 1996):

$$m_{l,r}(t) = k_f m_{l,r}^f(t), \quad (11)$$

with the constant factors $k_f = 0.5$ u/step.

Result: With a purely proportional controller the agent is able to compensate for only 35% of the external rotation of the drum ($\dot{\psi} = 1.0 \pm 1.3^\circ/\text{step}$). However, the control signal does not lead to an unstable behavior. The standard deviation is only slightly larger than with the proportional-integral controller.

4. Implementation on the robot

We implemented the controller on a mobile robot – the *KheperaTM* robot. The visual signals result from a small video camera with a conical mirror mounted above it (Chahl and Srinivasan, 1996). The optical axis of the video camera is oriented to the center of the cone. This configuration provides a 360° horizontal field of view extending from 10° below to 10° above the horizon (Franz, Schölkopf, Mallot, and Bühlhoff (in press)). The image is sampled on five circles along the horizon within a vertical aperture of 2.1° . The samples are averaged vertically to provide robustness against inaccuracies in the imaging system. Then the samples are horizontally lowpass

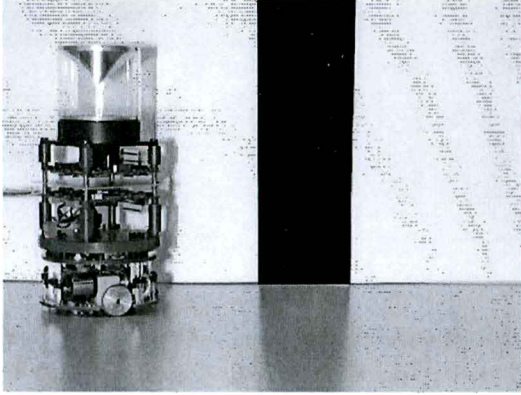


Figure 7 *KheperaTM robot with vision module. The optical axis of the camera is oriented vertically upwards, receiving mainly visual input from the image on the conical mirror.*

filtered using a Gaussian filter, resulting in 96 sensors on the horizontal ring, 48 for each eye. The resolution is higher than in the simulation.

Table 1 *Predictive coding: Weights of the lateral inhibition area with center pixel 0 and lateral pixels $\pm 3, \pm 2, \pm 1$ (obtained from 2000 images recorded during typical trajectories of the robot).*

pixel	0	± 1	± 2	± 3
weight	1.000	-0.510	0.003	0.007

For the processing of the video images, we model besides the temporal aspects of the LMCs, their spatial aspects by a spatial bandpass filter obtained by predictive coding – a procedure known for image compression (e.g., Gonzales and Woods, 1992). The weighting function of the filter is formed by three input units ($m=3$) in either direction. 1 gives an average filter characteristic that is obtained from 2000 images recorded during typical trajectories of the robot. The visual stimuli are then temporally highpass filtered and amplified. Filtering as well as motion detection are the same as in simulation.

The transmission weights that couple the outputs of the large field integration units β_l and β_r to the motor system are the same as in simulation (Eq. 7) and the control signals result from (Eq. 10). The constant factors are set to $k_f = 4.0$ mm/s and $k_{or} = 4.0 \cdot 10^{-3}$ mm/s. Intrinsic noise signals with a Gaussian distribution (Fig. 8) cause random rotations around the vertical axis. The velocity of the motors can be set stepwise to $\pm 8n$ mm/s with ($n = 1, \dots, 10$) for the left and right motor. The basic velocity is set to $v_0 = 40$ mm/s, which is modulated by the visual motion signals. The robot is updated at a rate of 12 Hz.

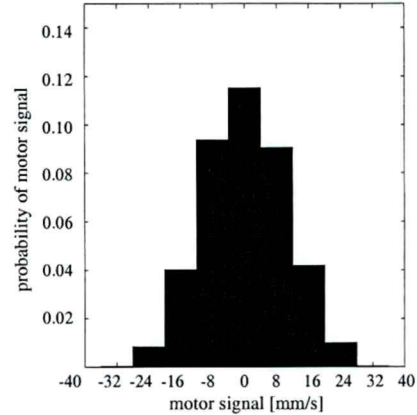


Figure 8 *Gaussian distribution of turning response due to the noise that is added to the motor signals.*

5. Experiments with the robot

5.1 Optomotor response behavior

Experiment: Similar to the fixation experiments with flies, in this experiment the robot is only able to turn around its vertical axis within a circular arena (diameter: 45 cm). For the optomotor response a pattern with black and white stripes is painted onto the wall of the arena ($\lambda = 51.4^\circ$). Instead of a constant rotatory bias of the drum, asymmetric motor signals are added to the left and right motor: ∓ 24 mm/s (this corresponds to $\dot{\psi} = \pm 4.2^\circ/\text{frame}$).

Result: In the case of an asymmetric motor signal that leads to a rotation of the robot about the vertical body-axis, the robot produces a compensatory turning response by the internally generated control signals compensating for 97% of the motor asymmetry (Fig. 9a).

5.2 Fixation behavior

Experiment: To test the fixation behavior, a single black stripe (angular width: 25.7°) is painted onto the white wall of the arena. The experiment is started with the stripe being at an orientation of $\psi = 57^\circ$ off the heading direction. Instead of measuring the absolute orientation of the robot in the drum, we used the visual angle of the stripe's retinal image.

Result: In an arena with a single black stripe, the robot is able to orient itself towards the stripe after about 8 s and fixate on it (Fig. 9b). This is in accordance with the result from the simulation.

5.3 Approach behavior

Experiment: In the next experiment the robot was started from various positions and with various orientations in the arena (Fig. 10). The robot has two degrees of freedom: translation in the heading direction and rotation around the vertical body-axis. The rotatory and

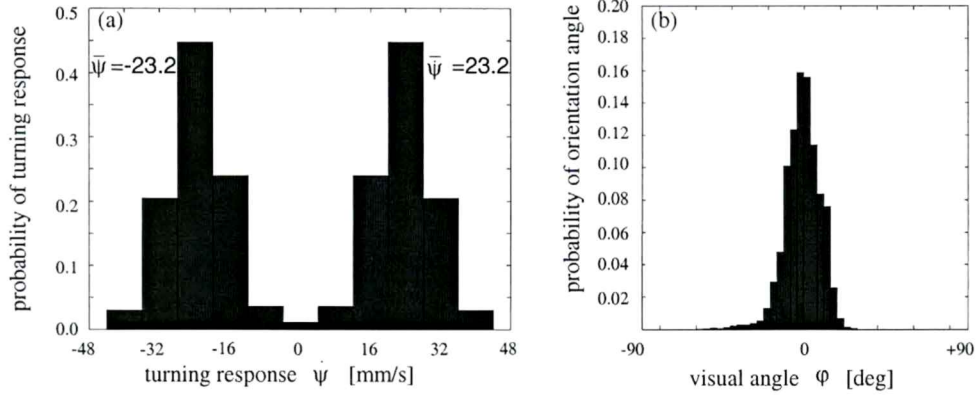


Figure 9 (a) Histogram of the optomotor response in the presence of a motor asymmetry of the left and right motor ($\mathbf{v}^a = (v_l^a, v_r^a) = (-24, +24)$ mm/s) (9700 steps). Compensatory motor signals of the left and right motor result in $v_l = 23.2 \pm 7.2$ mm/s and $v_r = -v_l$. (b) Histogram (9700 steps) of the visual angle φ of the stripe's retinal image: $\bar{\varphi} = -0.29^\circ \pm 10.36^\circ$.

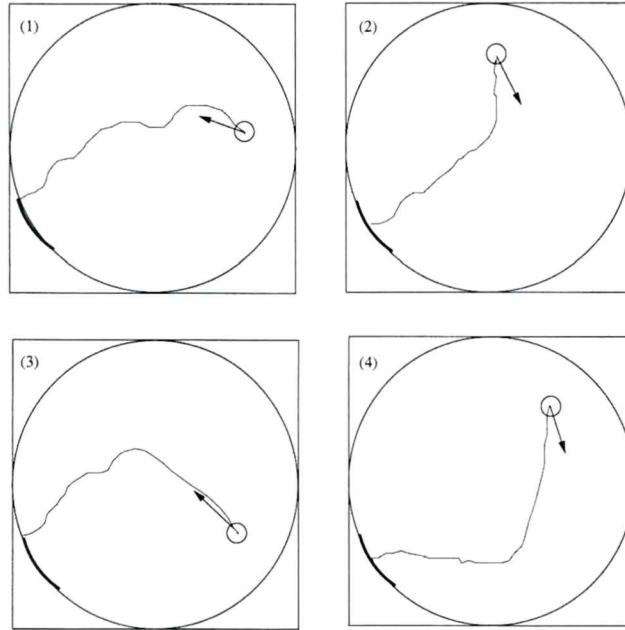


Figure 10 Approach of single stripe in an arena. The robot starts with the orientations relative to the center point of the stripe $\Delta\psi = -60^\circ, 60^\circ, 65^\circ, 70^\circ$.

translatory velocities are set according to Eq. 5.

Result: If the robot has two degrees of freedom, i. e. it is enabled to translate and rotate, it approaches the stripe in all cases (Fig. 10). The movement of the robot is guided by the motion that is perceived at the border of the stripe, because from the uniform black stripe no

motion information can be derived. Therefore, the agent approaches often one stripe instead of heading directly towards the middle of the stripe. The trajectories have been obtained by a visual tracking system, with a video camera recording the arena from a birds-eye view. The system tracks a red marker on top of the robot.

6. Discussion

We investigated whether one visuomotor controller is sufficient to generate both optomotor response and fixation behavior and we can in fact show that this is possible: The simulated agent as well as the *KheperaTM* robot show optomotor response and fixation behavior depending on the particular environmental conditions. In addition the robot approaches prominent objects in the arena if it is able to move around.

In order to explain the optomotor response, experimental results on flies suggest a temporal integration stage of the the output signals from the horizontal cells (Heisenberg and Wolf, 1984). We could show that for our agent the integration of the image motion signals leads to an optomotor response behavior comparable to that of flies. Purely proportional control signals are not sufficient to compensate for the drum's rotation. However, like in flies they do not lead to an unstable behavior, because of the motion detectors' response characteristic.

For the fixation of a single stripe, the following perceptual properties are essential: (i) an asymmetric response of the motion detectors to progressive and regressive motion, (ii) the spatial sensitivity function of the large field integration units with overlapping fields in front of the agent. The fixation behavior of the simulated agent is qualitatively comparable to that of flies.

The implementation of the control structure onto the robot was straight forward and the results show that the simulations represent the real world conditions of the robot very well. We slightly changed the proportionality factors of the proportional and integral parts of the controller. The robot is able to fixate on the black stripe as well as to stabilize the retinal image by optomotor response. With two degrees of freedom the robot even approaches the prominent object in the arena.

The implementation of our controller on an analog VLSI chip would be very useful for autonomous robots and for further studies of fly behavior. On such chips, motion detection mechanisms have been developed successfully (Sarpeshkar, Kramer, Indiveri, and Koch, 1996; Harrison and Koch, 1998). These chips integrate both the photosensors and the motion computation on a single chip. Like in biological systems, a parallel processing of visual signals is thus possible. Although the sensors on the chips show a poor signal-to-noise ratio, and the performance decreases significantly at low contrast and low illumination levels. For the simulation of biological processes this does not have to be a disadvantage, as noise is intrinsic in all biological neural systems.

7. Conclusions

The comparison of the results with investigations in flies suggests that the large field cells most probably participate in mediating both the optomotor response and the fixation behavior. Further investigations of the robot's

behavior under various experimental conditions have to be done to compare its behavior in more detail with that of flies. It is known from investigations on flies that the large field cells alone are not responsible for the object fixation behavior. Full object fixation is mediated by the contribution of other cells, for example the small field cells (Egelhaaf, 1985) which respond selectively on motion in small parts of their receptive field. In future work our model may be extended by adding small field units.

Our controller has important implications for the design of autonomous agents with a behavior based control architecture. There is one fundamental problem for the design of behavior-based architectures. The design of the agent's architecture involves the definition of a basic set of behaviors that enables the agent to accomplish a given task. The designer has to predict all possible interactions between behavioral modules and the environment. Thus the decomposition of the agent's architecture into behavioral modules has to be done very carefully. As we showed here, in some cases it is not necessary to realize separate modules for different behaviors. Our controller regulates both the optomotor response and the fixation behavior. Which of the two behaviors predominates, depends on the particular environment. Therefore, a further detailed understanding of the functionality of sensorimotor processes in biological systems would be very useful for the development of control algorithms for autonomous robots.

Acknowledgments: This work was done in close collaboration with M. O. Franz whom we thank for his interest and valuable criticism. We would also like to thank H. Krapp and A. Borst for stimulating discussions on fly vision and helpful comments on preliminary versions of this article. A longer and more detailed version of this article, in which further tests of the controller are described, is submitted to 'Robots and Autonomous Systems'.

References

- R. D. Beer (1990). *Intelligence as Adaptive Behavior*. Academic Press, San Diego, CA.
- R. A. Brooks (1986). A robust layered control system for a mobile robot. *IEEE J. Robot. and Aut.*, 2(1):14 – 23.
- H. Bülthoff (1982). *Drosophila* mutants disturbed in visual orientation (ii.). *Biol. Cyb.*, 45:71 – 77.
- D. T. Cliff (1992). Neural networks for visual tracking in an artificial fly. In *Proc. 1st Europ. conf. on Art. Life*, pages 78 – 87, Cambridge, MA, MIT Press.
- H. Cruse, C. Bartling, G. Cymbalyk, J. Dean, and M. Deifert (1995). A modular artificial neural network for controlling a 6 – legged walking system. *Biol. Cyb.*, 72:421 – 430.
- A. P. Duchon and W. H. Warren (1994). Robot navigation from a gibsonian viewpoint. In *Proc. IEEE Int. Conf. Systems, Man and Cyb.*, pages 2272 – 2277, Piscataway, NJ, 1994. IEEE.
- M. Egelhaaf (1985). On the neural basis of figure – ground

- discrimination by relative motion in the visual system of the fly (ii.). *Biol. Cyb.*, 52:195 – 209.
- M. Egelhaaf and A. Borst (1993). Motion computation and visual orientation in flies. *Comp. Biochem. Physiol. A*, 104(4):659 – 673.
- J. D. Foley, A. van Dam, S. K. Feiner, and J. F. Hughes (1987). *Computer graphics – principles and practice*. Addison–Wesley, Reading, MA.
- N. Franceschini, J. M. Pichon, and C. Blanes (1992). From insect vision to robot vision. *Phil. Trans. R. Soc. Lon. B*, 337:283 – 294.
- M. O. Franz, B. Schölkopf, M. A. Mallot, and H. H. Bülthoff (in press). Learning view graphs for robot navigation. *Aut. Robots*.
- R. C. Gonzales and R. Woods (1992). *Digital image processing*. Addison – Wesley, Reading, MA.
- K. G. Götz (1964). Optomotorische untersuchung des visuellen systems einiger augenmutanten der fruchtfliege *drosophila*. *Kybernetik*, 2(2):77 – 92.
- K. G. Götz (1975). The optomotor equilibrium of the *drosophila* navigation system. *J. Comp. Physiol.*, 99:187 – 210.
- K. G. Götz and H. Wenking (1973). Visual control of locomotion in the walking fruitfly *drosophila*. *J. Comp. Physiol.*, 85:235 – 266.
- R. R. Harrison and C. Koch (1998). An analog vlsi model of the fly elementary motion detector. In *Advances in Neural Information Processing Systems 10*, San Mateo, CA, Morgan Kaufman Publishers.
- M. Heisenberg and R. Wolf (1984). *Vision in Drosophila*. Springer Verlag, Berlin.
- J. M. Missler and F. A. Kamangar (1995). A neural network for pursuit tracking inspired by the fly visual system. *Neural Networks*, 8(3):463 – 480.
- F. Mondada, E. Franzi, and P. Ienne (1994). Mobile robot miniaturization: A tool for investigation in control algorithms. In *Proc. 3rd Int. Symp. Exp. Robotics*, London, Springer Verlag.
- W. Reichardt and T. Poggio (1976). Visual control of orientation behavior in the fly. part 1: A quantitative analysis. *Quart. Reviews Biophysics*, 9(3):311 – 375.
- R. Sarpeshkar, J. Kramer, G. Indiveri, and C. Koch (1996). Analog vlsi architectures for motion processing: From fundamental limits to system applications. 84(7):969 – 982.
- N. Tinbergen (1953). *Instinktlehre – vergleichende Erforschung angeborenen Verhaltens*. Parey Verlag, Berlin, Hamburg.
- A.-K. Warzecha and M. Egelhaaf (1996). Intrinsic properties of biological motion detectors prevent the optomotor control system from getting unstable. *Phil. Trans. R. Soc. Lon. B*, 351:1579 – 1591.
- B. Webb (1995). Using robots to model animals: a cricket test. *Robotics and Aut. Systems*, 16:117 – 134, 1995.
- K. Weber, S. Venkatesh, and M. V. Srinivasan (1997). Insect inspired behaviours for the autonomous control of mobile robots. In S. Venkatesh M. V. Srinivasan, editor, *From living eyes to seeing machines*, Oxford, New York, Tokio, Oxford University Press.